

Mineral Dissolution, Precipitation, and Ion Exchange in Surfactant Flooding

The transient retention of an anionic surfactant below the critical micellar concentration flowing in an argilo-calcareous sandstone is shown to depend mainly upon: (1) the dissolution of trace amounts of calcium carbonate contained in the sandstone and (2) precipitation and redissolution of the surfactant with calcium ions due to carbonate dissolution or ion exchange on the clays. The adsorption process on solid surfaces is secondary, due to a high pH resulting from the presence of carbonates. A predictive model is developed. It is compared with typical surfactant breakthrough curves and demonstrates that dissolution of calcite is the main process affecting the transport of surfactant close to the injection point.

**R. Krebs, M. Sardin,
D. Schweich**

Laboratoire des Sciences
du Génie Chimique-CNRS
F-54042 Nancy Cedex, France

Introduction

Among the many physicochemical interactions that affect the efficiency of chemical flooding in enhanced oil recovery (EOR) processes, the retention of surfactant is considered to be the most crucial. For many years the adsorption of anionic surfactants on the surface of minerals has been considered to be the main explanation for this retention (Trogus et al., 1977; Somasundaran et al., 1977). The sensitivity of this adsorption process to the concentration of multivalent ions (Figdore, 1982) indicates the effect of three other physicochemical processes

1. Precipitation of the surfactant by the multivalent ions (Celik et al., 1979, 1982; Zundel and Siffert, 1985; Bavière et al., 1983)

2. Cation exchange on the clays, which at least releases calcium (Pope et al., 1978; Griffith, 1978; Smith, 1978; Hirasaki 1980, 1982)

3. Solubilization of trace amounts of calcite, which ensures the resaturation of clays with calcium (Schweich, 1985; Schweich and Sardin, 1985).

Up to now, particularly in well-defined laboratory conditions, the experimental studies of these processes coupled with flow have been very limited. Only Bourdarot and Sardin (1985) and Bourdarot et al. (1984) have shown that cation exchange governs the efficiency of a microemulsion and the trapping of the surfactant in the residual oil. However no column experiment has been carried out to study the respective importance of each process in the transport of an anionic surfactant, and modeling is

partly based on an empirical description of the retention of the surfactant.

Several authors have also recognized the importance of mineral dissolution, although this process is taken into account empirically in most studies. Hirasaki (1982) and Chan and Kremesec (1985) have modeled the dissolution process through a fictitious concentration of divalent cations in the feed. Jensen and Radke (1985) have had to invoke a fictitious concentration of sodium hydroxide in the feed to accurately model the pH during transport of alkaline buffers in Berea sandstone. In many situations mineral dissolution is due to carbonates, which increase the concentration of divalent cations and the pH. Even in sandstones that contain trace amounts of carbonates (Berea, Chateaufort, Gue sandstones) equilibration between deionized water and sandstone in a column results in a pH as high as 9 to 10 (Jensen and Radke, 1985; Schweich and Sardin 1985). This high pH is known to reduce the amount of adsorbed surfactant (Trogus et al., 1977; Goddard and Somasundaran, 1976) and one may wonder whether this adsorption process is really important in these situations.

In soil science, similar problems are encountered in modeling pollution by heavy metal ions and assessing nuclear waste disposals (OECD-NEA, 1983). New models taking into account the fundamental solid-fluid interaction mechanisms and the competition between species are now being developed (Walsh et al., 1984; Miller and Benson, 1983). However, careful laboratory experiments must be done to identify the processes affecting the species under study (Sardin et al. 1986).

This paper describes the modeling and the experimental study of the transport of an anionic surfactant (sodium *n*-paraocetyl-

Correspondence concerning this paper should be addressed to D. Schweich.

benzene sulfonate) in a sandstone similar to that of the French EOR pilot plant at Chateaufort. The objectives are:

1. To propose a model describing the movement of the surfactant, taking mineral dissolution into account. The main mechanisms that will be considered are ion exchange and the precipitation and dissolution of calcite and surfactant; adsorption is shown to be secondary.

2. To show the respective importance of each of the processes mentioned above in the migration of a surfactant slug below the critical micellar concentration (CMC) in the absence of oil.

Modeling of Interactions

Assumptions

The model is based on the following assumptions.

- Calcium/sodium ion exchange on the clays; solubilization of limestone and precipitation of the surfactant are taken into account; the precipitated surfactant is stationary.

- Adsorption of surfactant molecules, anion exchange, migration of solid particles and complexation of ions are neglected

- Micellization is excluded

- The phases are incompressible, isothermal, and in thermodynamic equilibrium

- Solutions are ideal

- Fluid velocity is constant and the fluid flow is one-dimensional

- The porous matrix is uniform in space

- Hydrodynamic dispersion is represented by the model of mixing cells in series

- Outside the porous matrix the feed solutions are in thermodynamic equilibrium with atmospheric CO₂; on the other hand, neither the fluid nor solid phase is in contact with air inside the column

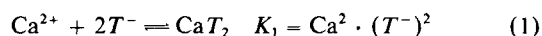
- Calcium carbonate is always present in the porous matrix; complete dissolution by the fluid flow is excluded

The concentrations of ions or molecules are denoted by their chemical symbols with the exception of the surfactant anion, which is abbreviated by T^- . Cations fixed at the liquid-solid interface (\bar{Na}^+ , \bar{Ca}^{2+}) are distinguished from cations in solution (Na^+ , Ca^{2+}) by overbars.

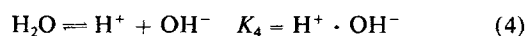
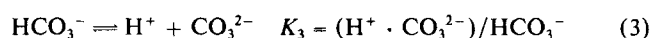
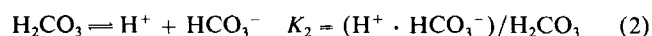
Chemical equilibrium relationships

From the assumptions made above the following chemical reactions and relationships for local chemical equilibrium are deduced:

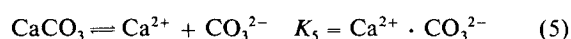
Precipitation of the surfactant



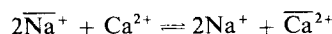
Ionizations of carbonic acid and water



Dissolution of calcium carbonate



Cation exchange



$$K_6 = (\bar{X}_{Ca}/Ca^{2+}) \cdot (Na^+/\bar{X}_{Na})^2 \quad (6a)$$

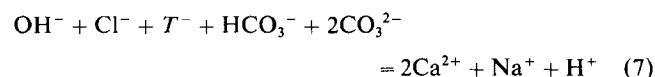
$$\bar{N}_E = \text{constant} \quad (6b)$$

where respectively \bar{X}_{Na} and \bar{X}_{Ca} are the molar fractions of cations Na^+ and Ca^{2+} on the solid phase.

Looking at the solubilities of different surfactants below the critical micellar concentration (Peacock and Matijevic, 1980), the precipitation of surfactant may be represented by a single reaction. Equation 1 only applies when solid CaT_2 exists. For a constant fraction of CO₂ in the atmosphere (0.3%) the concentration of H₂CO₃ in the feedstocks is 1.2×10^{-5} mol/L. Following Pope et al. (1978), Hirasaki (1982), and Bolt (1982), the ion exchange process between the soil surface and the bulk flow is represented by a simple mass action law model. The selectivity constant K_6 as well as the total exchange capacity \bar{N}_E are assumed to be constant.

Supplementary algebraic relationships

Electroneutrality of the fluid and solid phase yields:



$$\bar{Na}^+ + 2\bar{Ca}^{2+} = \bar{N}_E \quad (8)$$

Furthermore, it has been shown (Schweich and Sardin, 1985) that the quantity I defined by:

$$I = 2H_2CO_3 + HCO_3^- + H^+ - OH^- \quad (9)$$

is constant with respect to space and time. The numerical value of I is calculated from the composition of the solutions in the feedstock by means of Eqs. 2, 3, and 4; the calculated value of I used in this work is included in Table 1.

Mass balance equations

The precipitation process coupled with many chemical reactions at equilibrium prevents the use of the method of characteristics, although it has been applied successfully in similar problems (Hirasaki, 1982; Klein, 1986). The mass balance equations are solved numerically and this allows one to account for hydrodynamic dispersion, which is represented by the model of mixing cells in series. Algebraic Eq. 1 to 9 include 12 unknown concentrations (five anions: HCO_3^- , CO_3^{2-} , T^- , Cl^- , OH^- ; five cations: H^+ , Na^+ , Ca^{2+} , \bar{Na}^+ , \bar{Ca}^{2+} ; two uncharged molecules: H_2CO_3 , CaT_2). Consequently, three mass balance equations are required for each mixing cell k . The concentrations of chloride, surfactant, and sodium are chosen as independent unknown concentrations.

$$QCl_{k-1} = QCl_k + \frac{V_0}{J} \frac{dCl_k}{dt} \quad (10)$$

$$QT_{k-1} = QT_k + \frac{V_0}{J} \left(\frac{dT_k}{dt} + 2 \frac{dCaT_{2k}}{dt} \right) \quad (11)$$

$$QNa_{k-1} = QNa_k + \frac{V_0}{J} \frac{dNa_k}{dt} + \frac{M}{J} \frac{d\bar{Na}_k}{dt} \quad (12)$$

The concentration of precipitated surfactant is defined as the number of moles of CaT_2 per unit volume of the fluid phase. V_0 , Q , and M are respectively the pore volume, the constant volumetric flow rate, and the mass of sandstone in the column. The number of mixing cells J is related to the hydrodynamic dispersion coefficient D by (Villermaux, 1982):

$$(u \cdot L)/D = 2(J - 1) \quad (13)$$

The system of $3 \cdot J$ ordinary differential equations, Eqs. 10, 11, and 12, is integrated numerically by means of Euler's method. For this purpose the algebraic equations, Eqs. 1–9, are rearranged. For comparison with experimental data, the eluted volume V is substituted for the time t :

$$V = Q \cdot t \quad (15)$$

As a result, breakthrough curves for each species are calculated.

Experimental Details

Test facility and operating method

A glass tube of 25.4 mm ID was packed with the sandstone (from Gue) to form a column 150 to 250 mm high. This sandstone is from an outcrop of the sediment layer of the French oil field of Chateaufrenard. The Gue sandstone consists of 95% quartz, 2 to 3% clays (mainly kaolinite), and 1% limestone. Particles were less than 0.4 mm dia., with an average diameter of 0.125 mm.

As shown in Figure 1, various feed solutions (H_2O , NaT , or $NaCl$) could be pumped to the column. One of the anionic surfactants studied was sodium *n*-paraocetylbenzene sulfonate [$CH_3-(CH_2)_7-C_6H_4-SO_3Na = NaT$] with a Kraft point of 18°C. A flow rate of about 0.2 mL/min was used so as to approach thermodynamic equilibrium between the fluid and the solid phases. The effluent was sampled by a fraction collector, each fraction representing about 20% of the pore volume. The test facility, Figure 1, was held at constant temperature inside a drying oven.

The sequence of injections is illustrated in Figure 2. After equilibrium of the sandstone with demineralized water, the surfactant NaT was injected ($t = 0$, $V = 0$) at a concentration C_0 . The surfactant slug, usually two pore volumes long, was fol-

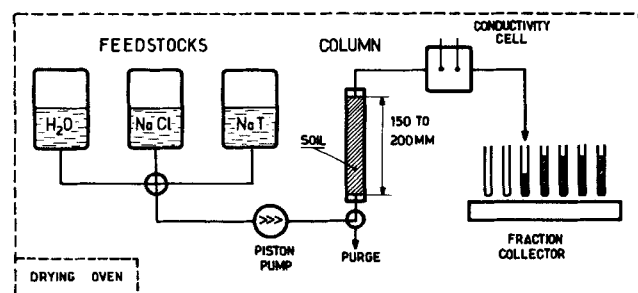


Figure 1. Test facility for consecutive injection of water, surfactant (NaT), and $NaCl$ in a soil column.

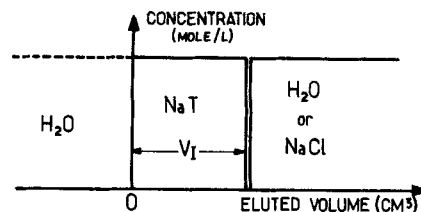


Figure 2. Composition in feed stream vs. reduced volume.

lowed either by demineralized water or by a sodium chloride solution for runs at high surfactant concentrations. Finally, to restore the initial calcium saturation of clays, calcium chloride was injected after each run.

Analytical procedures

After a run the eluted volume V was determined by the weight of the collected fractions. The concentration of each species was very sensitive to other ions in solution and to washed-out particles. The surfactant anion T^- was quantitatively analyzed by UV spectrometry (peak at 254 nm). The fractions were centrifuged to separate noncolloidal clay particles. Then the spectra were corrected for the contribution of the remaining colloids. The correction procedure was checked by chemical analysis (Reid et al., 1967). The atomic absorption spectrometric analysis of Na^+ and Ca^{2+} ions was disturbed by the surfactant. Therefore T^- was precipitated by an excess of barium chloride and centrifuged as BaT_2 . To account for interferences between barium and Na^+ and Ca^{2+} ions, the calibration solutions for the atomic absorption measurements contained the same amount of barium as the diluted fractions.

Operating conditions and model parameters

Table 1 gives the operating conditions and the numerical values of the parameters characterizing the system Gue sand/sodium *n*-paraocetylbenzene sulfonate. The model involves nine parameters: K_1 , K_2 , K_3 , K_4 , K_5 , K_6 , \bar{N}_E , V_0 , J . The solubility product of the calcium salt CaT_2 found in the literature (Zundel and Siffert, 1984) was confirmed by our own batch experiments. The equilibrium constants of the ionization reactions K_2 , K_3 , and K_4 were taken from Olive (1978) and Al Droubi et al. (1978). Further parameters describing chemical interactions, such as the solubility product of calcium carbonate K_5 , the selectivity constant for ion exchange K_6 , and the total exchange capacity \bar{N}_E , were determined by suitable soil column experiments (Schweich and Sardin, 1985). The numerical value of the selectivity factor K_6 , Table 1, is in close agreement with data found by other authors (Bruggenwert and Kamphorst, 1982; Chan and Kremesec, 1985; Hirasaki, 1982) for similar types of soils.

The pore volume V_0 and the number of mixing cells J were obtained from residence time distribution measurements.

Interpretation of Experimental Results

Elution curves for $T^-(V/V_0)$, $Na^+(V/V_0)$, and $Ca^{2+}(V/V_0)$ are shown in Figures 3–6. For runs 1 and 2 shown in Figures 3 and 4, the surfactant slug was driven by water. For runs 3 and 4 $NaCl$ solutions at the same concentration as the surfactant were substituted for water.

At the lowest feed concentration, run 1, Figure 3, the surfactant behaves as a perfect tracer. Front broadening is essentially

Table 1. Operating Conditions and Parameters for Gue Sand/*N*-paraoctylbenzenesulfonate System

| Variable Parameters | Constant Parameters | | | | |
|---|----------------------|----------------------|----------------------|---|----------------------|
| | 1 | 2 | 3 | 4 | 5 |
| Q , 0.2 cm ³ /min | | | | | |
| K_1 , 1.0×10^{-9} mol ³ /L ³ | | | | | |
| K_2 , 4.13×10^{-7} mol/L | | | | | |
| K_2 , 4.19×10^{-11} mol/L | | | | | |
| | | | | K_4 , 6.62×10^{-15} mol ² /L ² | |
| | | | | K_5 , 7.19×10^{-9} mol ² /L ² | |
| | | | | K_6 , 6.3 mol/L | |
| | | | | I , Eq. 9, 2.845×10^{-5} mol/L | |
| Run | | | | | |
| Variable Parameters | 1 | 2 | 3 | 4 | 5 |
| C_0 , mol/L | 10^{-3} | 2×10^{-3} | 5×10^{-3} | 10^{-2} | 2×10^{-2} |
| V_i/V_0 | 1.13 | 2.04 | 2.03 | 2.07 | 2.11 |
| Temp., °C | 20 | 20 | 20 | 20 | 35 |
| M , kg | 0.161 | 0.140 | 0.146 | 0.146 | 0.146 |
| L , cm | 19.5 | 17.6 | 19.5 | 19.5 | 19.5 |
| \bar{N}_E , eq/kg | 8.4×10^{-3} | 8.4×10^{-3} | 8.4×10^{-3} | 5.75×10^{-3} | 3.2×10^{-3} |
| V_0 , cm ³ | 45.2 | 37.9 | 42.7 | 42.9 | 42.9 |
| J | 200 | 190 | 260 | 260 | 260 |
| Drive | Water | Water | NaCl | NaCl | NaCl |
| Recovered T^- , % | 105.1 | 96.25 | 96.7 | 111.2 | 103.8 |

caused by hydrodynamic dispersion. As already described in Schweich and Sardin (1985), a peak of Ca^{2+} followed by a peak of Na^{+} is observed. These peaks are a consequence of the competition between ion exchange and limestone solubilization. For the sake of simplicity the $\text{Ca}^{2+}/\text{Na}^{+}$ peak sequence observed for all runs, Figures 4, 5, and 6, will not be discussed further.

At a feed concentration of 2×10^{-3} mol/L run 2, Figure 4, the first front ($1 < V/V_0 < 3$) of the T^- breakthrough curve consists of two parts:

1. A sharp subfront ($0 < T^- < 10^{-3}$ mol/L), already seen in Figure 1, where only hydrodynamic dispersion occurs
2. A leading subfront ($10^{-3} < T^- < 2 \cdot 10^{-3}$ mol/L) where calcium ions supplied by clays and limestone have precipitated a fraction of the surfactant

Along the leading subfront T^- and Ca^{2+} concentrations satisfy Eq. 1. This supports the affirmation that the precipitation process is at equilibrium.

At a feed concentration of 5×10^{-3} mol/L run 3, Figure 5, T^- concentrations in the spreading front ($1 < V/V_0 < 3$) do not reach the feed concentration. This indicates that a large fraction of the injected T^- precipitates. This fraction dissolves in the NaCl drive and induces the subsequent fronts [$V/V_0 > (V_0 + V_i)/V_0 = 3$] where two plateau zones must be distinguished. The first plateau zone is related to the peak of sodium, which exceeds the feed concentration of the NaCl drive. The second plateau zone is attended by a wide Ca^{2+} peak. A similar form of elution curves is shown in run 4, Figure 6, at a feed con-

centration of 10^{-2} mol/L. The second plateau zone is slightly longer than in run 3 because a larger amount of precipitate has to be dissolved. As for run 2, Ca^{2+} and T^{-} are in equilibrium with solid CaT_2 .

The qualitative explanations for the multiple fronts in the elution curves are obtained from:

1. The concentration profiles $T^-(x)$, $\text{Na}^+(x)$, $\text{Ca}^{2+}(x)$, and $\text{CaT}_2(x)$ sketched in Figure 7E for runs with the NaCl drive
2. The equilibration process between the solution and the solid phase in the first cell of the column model.

When the surfactant slug, Figure 7A, enters this cell at a high concentration, a fraction of the surfactant precipitates with calcium generated by calcite dissolution and exchange on clays. Although the amount of exchangeable calcium is limited, calcite is supposed to be an infinite source of calcium. Consequently, the higher the surfactant concentration, the higher the amount of surfactant precipitated by calcite dissolution. This amount of precipitate increases continuously, Figure 7D ($0 < V < V_I$), until dissolution by the NaCl drive begins, Figure 7D ($V > V_I$). Downstream of the first cell, the resulting feed in the column is a slug flanked with a more or less long plateau zone of surfactant in equilibrium with calcium, Figure 7B. The larger the amount of surfactant precipitated, the longer this plateau zone in Figure 7B.

The profiles, Figure 7E, are divided into five sections. In each section different interaction mechanisms predominate.

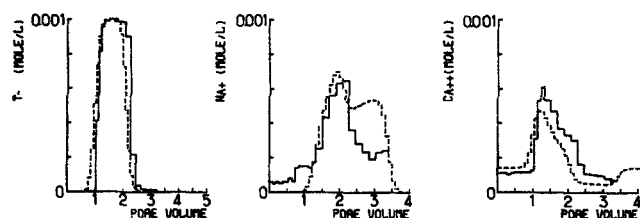


Figure 3. Run 1: injection of 1.13 pore volumes of surfactant at 10^{-3} mol/L driven by water.
Surfactant anion behaves nearly as a perfect tracer.
— experiment; --- model

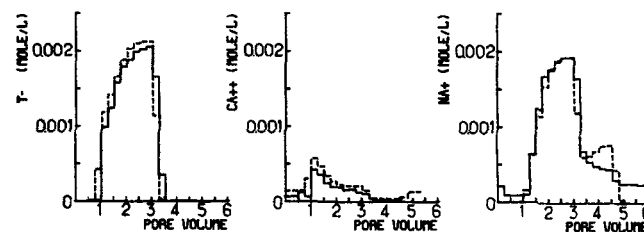


Figure 4. Run 2: injection of 2.04 pore volumes of surfactant at $2 \cdot 10^{-3}$ mol/L driven by water.
Slight precipitation of surfactant with Ca^{2+} ions detached from clays by ion exchange with Na^+
— experiment; --- model

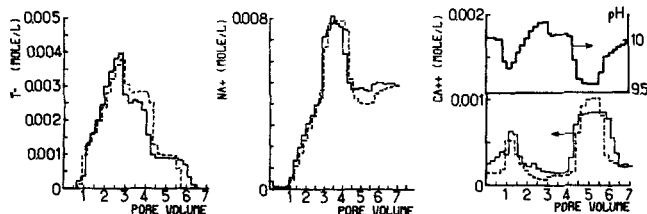
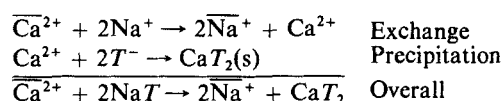


Figure 5. Run 3: injection of 2.03 pore volumes of surfactant at $5 \cdot \text{mol/L}$ driven by NaCl.

Multiple concentration fronts for surfactant dissolution
— experiment; --- model

In section I only limestone is dissolved in the initial water. Therefore T^- and Na^+ concentrations are zero.

Section II corresponds to the injection of the surfactant slug (first front of Figure 7B or 7A). The surfactant profile is composed of two fronts. In the first (downstream) front only cation exchange occurs and calcium concentration increases going upstream. In the second front (upstream part of section II) the surfactant precipitates with calcium exchanged with the clays by sodium. Consequently calcium concentration decreases going upstream. The overall process results from two particular mechanisms:



As a result NaT is consumed whereas CaT_2 is produced, while solubilization of calcite is secondary.

Sections III and IV of Figure 7E correspond to the solubilization of CaT_2 in the NaCl drive. At the rear end of section III, the above reactions are reversed. Ca^{2+} ions released by the dissolution of CaT_2 are exchanged against sodium ions fixed previously on the clays. The exchanged sodium is added to the NaCl drive and an excess peak widens from its upstream part. Since Ca^{2+} ions are consumed by the ion exchange process, the equilibrium concentration of T^- is allowed to be quite high. Two fronts of T^- are observed, one associated with the unretained chloride (downstream) and another with a dissolution wave (upstream). In this section dissolution of CaT_2 is favored by the clays, which act as a calcium sink, and the dissolution of calcite is secondary.

Section IV is mainly due to the tail in the surfactant history at the outlet of the first cell, Figure 7B. This tail is composed of calcium and surfactant at equilibrium with CaT_2 . This feed solution prevents any complete dissolution of the downstream

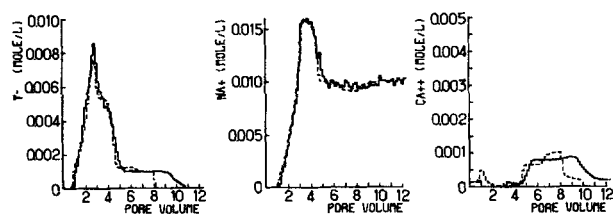


Figure 6. Run 4: injection of 2.07 pore volumes of surfactant at 10^{-2} mol/L driven by NaCl.

Long dissolution plateau zone.
— experiment; --- model

precipitate in section III. When pure NaCl appears at the outlet of the first cell, the second dissolution wave is created and appears at the rear of section IV. This means that the greater the amount of precipitated surfactant in the first cell, the longer section IV will be. As in sections II and III, the dissolution of calcite is secondary.

In section V, CaT_2 has completely dissolved. Only limestone solubilization in the NaCl drive remains.

This analysis suggests that a concentrated surfactant solution (below CMC) is affected by calcium according to two distinct processes:

1. Close to the column inlet (first cell of the model) the equilibration of the feed with calcium generated by the dissolution of calcite is the main retention mechanism; since calcite is always present, the amount of precipitate increases continuously with the concentration of the feed.

2. Inside the column the main mechanisms are cation exchange on the clays and CaT_2 precipitation/dissolution. Contrary to the precipitation of T^- with calcium ions from calcite, the amount of precipitated surfactant inside the column is limited by the exchangeable calcium; as long as solid CaT_2 remains in the column, dissolution of calcite is secondary.

Comparison and Discussion

The elution curves calculated by means of Eqs. 1–12 match the experimental data for all runs. The location of the different concentration fronts, the peak heights, and the concentration levels of the plateau zones are well estimated except for the tail of sodium in runs 1 and 2. The good agreement was obtained with model parameters found in literature or determined by suitable experimental procedures, avoiding any parameter fitting to experimental data of runs 1, 2, and 3. This supports the affirmation that the proposed elementary processes are the main controlling mechanisms in a surfactant/soil system of the argillo-calcareous type when there is no clay migration. The basic model assumptions—local thermodynamic equilibrium, no adsorption—seem justified. In the concentration range studied, the remaining discrepancies between experimental data and predictions are due either to second-order processes (surface adsorption, dissolution kinetics) or to other important mechanisms: soil migration and micellization.

Adsorption of the surfactant anion

A great deal of work has been done emphasizing the important role of surface adsorption of the surfactant (Somasundaran and Hanna, 1977; Trogu et al., 1977; Celik et al., 1979; Goddard and Somasundaran, 1976; Scamehorn et al., 1982). This mechanism should be observed in the absence of precipitation as in run 1, Figure 3, and the beginning of breakthrough in run 2, Figure 4. However, only a slight retention of the T^- ion with respect to a perfect tracer is observed. This indicates that the surface adsorption mechanism is secondary, although it is probably the reason for the retention mentioned above.

No continuous pH measurements have been done. However the pH of the outlet fluid for a feed of deionized water was found to be about 9.5 because of dissolution of calcium carbonate. This experimental result is in agreement with the pH found on a Berea sandstone by Jensen and Radke (1985); it also agrees with the calculated pH illustrated in Figure 5, which shows that pH is always in the range 9.7–10.4. Many adsorption studies

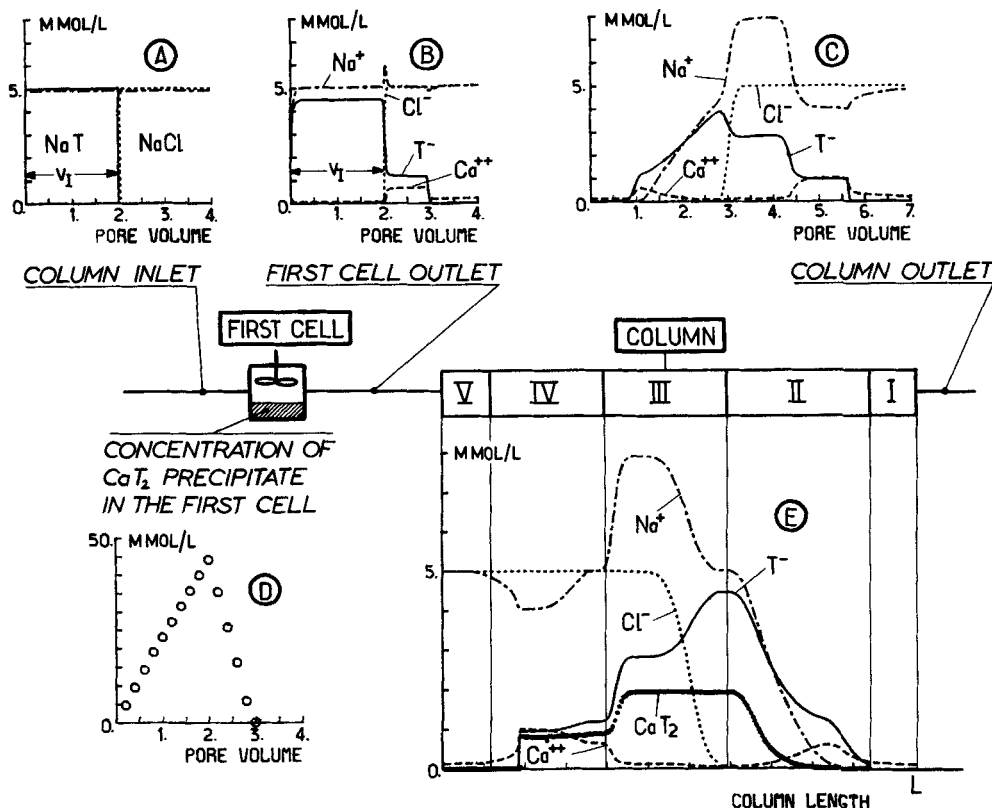


Figure 7. Typical concentration profile in a column of infinite length.

A. Feed solution history; B. History in first cell; C. Outlet of column; D. Amount of precipitate in first cell; E. concentration profiles

(Goddard and Somasundaran, 1976; Figdore, 1981) show that adsorption of anionic surfactants is very weak for this pH range. Therefore adsorption is secondary in every experiment provided there is a slight amount of carbonate that dissolves and acts as a buffer which maintains a high pH. Hirasaki (1982) and Chan and Kremesec (1985) have studied surfactant transport with mineral dissolution. To account for the observed surfactant fronts they introduced an empirical adsorption isotherm in their models. Provided that the mineral dissolution they observed is carbonate dissolution, our results show that the precipitation/dissolution of the surfactant monomer is probably more appropriate than adsorption to explain the surfactant retention.

It could be argued that increasing the amount of clay would increase the amount of adsorbed surfactant. However, the larger the amount of clay, the larger the amount of exchanged calcium and the larger the amount of precipitated surfactant. As a consequence the competition between adsorption and precipitation would remain qualitatively unchanged. Finally, similar experiments with sodium 4-dodecylbenzene sulfonate (4DBSNa) have been carried out and similar results have been obtained. Although the coverage of mineral surfaces by surfactant molecules occurs at a lower concentration for 4DBSNa than for the sodium *n*-paraocetylbenzene sulfonate (npOBSNa), the solubility product of the surfactant is lower for (4DBS)₂Ca than for (npOBS)₂Ca. Once more this results in a retention essentially due to precipitation rather than adsorption. It may be that many results by other investigators on the same problem could be reinterpreted in terms of precipitation based on a known solubility

product instead of an empirical adsorption process with fitted parameters.

Dissolution kinetics of CaCO₃

At low feed concentrations—runs 1 and 2, Figures 3 and 4—and pore volumes corresponding to the breakthrough of the water drive, the experimental values for Ca²⁺ fall above the theoretical values, whereas the Na⁺ concentrations fall below. As already suggested in Schweich and Sardin (1985) this may be due to a kinetically controlled solubilization process of CaCO₃. Otherwise the predictions based on the equilibrium assumption are satisfactory for the chosen flow rate, Table 1. The agreement should be better in an oil field far from the injection well, where fluid velocities are smaller than in these experiments. Close to the injection well, the dissolution kinetics of CaCO₃ will slow down the equilibration of the surfactant solution with calcium ions. The amount of precipitated CaT₂ will not be reduced but it will spread over a larger volume than that corresponding to the first cell of the model. In actual processes this would prevent pore clogging.

Clay particle migration

Reduction of clay migration was the reason the water drive was replaced by a NaCl drive with the same feed concentration as the surfactant slug. Clays fixed by weak forces on other solid particles are dispersed by changes in the ionic strength. This process has been observed for runs 4 and 5 (see below). Sus-

pended clay particles were found in the collected fractions corresponding to the first front and the first plateau zone of surfactant. As a result the exchange capacity was reduced during the experiment (26% in run 4) and the recovery rate of T^- was too high due to analytical uncertainties, Table 1. The theoretical curves in Figure 6 are those obtained with the reduced value of \bar{N}_E measured after the run. Any attempt to fit the experimental curves with the exchange capacity before run 4 gave poor results. This is unfortunate because, regarding present knowledge of clay dispersion and clay migration mechanisms, accounting for these effects in a compositional model is not very promising. No clay migration occurs with NaCl slugs at the same concentration as the surfactant solution. This allows one to measure the exchange capacity after each run, Table 1, runs 4 and 5. Although we claim that adsorption is secondary in the retention process of the surfactant, we consider that it must be accounted for to explain the different dispersion behavior of the clays in surfactant (4DBSNa or npOBSNa) or NaCl solutions.

Micellization

The model does not include micellization, which is known to considerably alter the precipitation mechanism of CaT_2 (Hirasaki, 1982; Chan and Kremesec, 1985). Therefore it is restricted to surfactant concentrations below the critical micellar concentration ($CMC = 1.2 \times 10^{-2}$ mol/L for pure npOBSNa solutions). Figure 8, run 5, shows experimental and calculated elution curves $T^-(V/V_0)$ at a feed concentration of 2×10^{-2} mol/L, which is above the CMC. As long as the concentration of T^- remains below the CMC the model correctly predicts the leading front due to precipitation, but it fails above the CMC. The experimental tail is much shorter than the theoretical prediction. Batch experiments show that for a concentration of T^- greater than CMC, the solubility law described by Eq. 1 alone is no longer valid (Celik et al., 1979; Bavière et al., 1983; Zundel and Siffert 1985). The higher solubility, which can be modeled by Na/Ca exchange on the micelles (Hirasaki, 1982), will be included in the transport model and it will be the subject of a future publication.

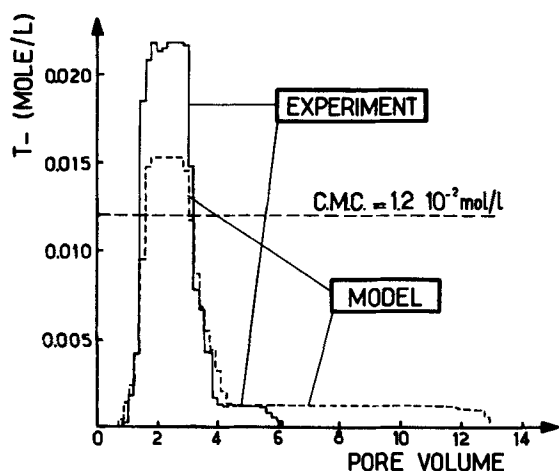


Figure 8. Run 5: injection of 2.11 pore volumes of surfactant at $2 \cdot 10^{-2}$ mol/L driven by NaCl.
Breakdown of model predictions due to surfactant micellization
— experiment; --- model

Conclusions

The above results show that:

1. The mass transport of two anionic surfactants (npOBSNa, 4DBSNa) below the CMC in a sandstone containing clays (2% wt./wt.) and limestone (1% wt./wt. calcite) is controlled by three coupled mechanisms: the dissolution of calcium carbonate, the sodium-calcium ion exchange on the clays, and the precipitation and redissolution of the calcic surfactant.
2. Ion exchange is not the only source of calcium. Solubilization of calcium carbonate is important and it must be inhibited to reduce the amount of precipitated surfactant and therefore its retention. This is achieved and proved by the success of the sodium bicarbonate preflush (Rivenq et al., 1985), for which an extension of the proposed model has been applied successfully.
3. Hirasaki (1982) and Chan and Kremesec (1985) have stipulated in their conclusions that dissolution needs to be accounted for. The proposed model gives a rigorous approach to this problem, taking into account carbonate dissolution.
4. Provided that carbonate dissolution occurs, the pH is above 9 and the adsorption of the anionic surfactant can be neglected.
5. The retention of the surfactant is essentially due to the precipitation/redissolution process of the surfactant monomer. The precipitated surfactant is supposed to be stationary and the amount of precipitate is governed by the solubility product, which can be measured by simple experiments. This avoids using an empirical adsorption isotherm with fitted parameters. Hirasaki and Chan and Kremesec could not use our approach since they neglected the concentration of surfactant monomer.
6. The precipitation of the surfactant by calcium carbonate occurs mainly at the inlet of the flow system. Subsequent precipitation due to the exchanged calcium occurs to a smaller extent inside the column.
7. Although the results are demonstrated for a given sandstone (Gue) they are valid for every sandstone containing trace amounts of carbonates (Berea sandstone).
8. The model should be improved to take into account the migration of clays and the ion exchange process on the micelles when they are present.

Acknowledgment

This work is part of the project Recupération améliorée du pétrole supported by the Ministère de la recherche et de l'industrie. R. Krebs acknowledges postdoctoral financial support from the Deutsche Forschungsgemeinschaft and the Ministère des relations extérieures.

Notation

Molar concentrations of ions or molecules are denoted by their chemical symbols with the exception of T^- (surfactant).

- Ca^{2+}, Na^+, \dots = cations in solution
 Ca^{2+}, Na^+ = cations fixed on solid ion-exchanger
 C_0 = molar concentration of feed solutions
 D = hydrodynamic dispersion coefficient
 J = number of mixing cells in series
 $K_{1..6}$ = equilibrium constants
 L = column length
 M = mass of soil in the column
 \bar{N}_E = ion exchange capacity
 Pe = Peclet number
 Q = volumetric flow rate
 t = time

T^- = molar concentration of surfactant anion
 u = fluid velocity
 V = eluted volume
 V_0 = pore volume
 V_f = volume of surfactant slug
 X = coordinate along column axis
 \bar{X}_{Na} , \bar{X}_{Ca} = molar fractions of cations Na and Ca on solid

Subscript

k = in mixing cell k

Literature Cited

- Al Droubi, A., J. L. Grondin, B. Fritz, and Y. Tardy, "Equilibres dans le système $\text{CaCO}_3 - \text{H}_2\text{O} - \text{CO}_2$," *Sci. Geol. Bull.* (Strasbourg), **31**(4), 195 (1978).
- Baviere, M., B. Bazin, and R. Aude, "Calcium Effect on the Solubility of Sodium Dodecyl Sulfate in Sodium Chloride Solutions," *J. Colloid Interf. Sci.*, **92**(2), 580 (1983).
- Bolt, G. H., ed., *Soil Chemistry. B: Physicochemical Models*, Elsevier, Amsterdam (1982).
- Bourdarot, G., and M. Sardin, "Chateaufrenard: échange d'ions, mécanismes de la récupération d'huile, rétention des tensio-acifs," *Solid-Liquid Interactions in Porous Media*, Technip, Paris 567 (1985).
- Bourdarot, G., M. Sardin, and A. Putz, "Chateaufrenard Field Test: Recovery Mechanisms and Interpretation," Paper SPE 12685, 4th Symp. EOR, Tulsa (Apr., 1984).
- Bruggenvert, M. G. M., and A. Kamphorst, "Survey of Experimental Information on Cation Exchange in Soil Systems," *Soil Chemistry. B: Physicochemical Models*, G. H. Bolt, ed., Elsevier, Amsterdam (1982).
- Celik, M. S., A. Goyal, E. Manev, and P. Somasundaran, "The Role of Surfactant Precipitation and Redissolution in the Adsorption of Sulfonate on Minerals," Paper SPE 8263, 54th SPE Ann. Fall meet., Las Vegas (Sept., 1979).
- Celik, M. S., E. D. Manev, and P. Somasundaran, "Sulfonate Precipitation-Redissolution-Reprecipitation in Inorganic Electrolytes," *AIChE Symp. Ser. No. 212*, **78**, 86 (1982).
- Chan, A. F., and V. J. Kremesec, "Cation Exchange in Porous Media with Broad-Equivalent-Weight Sulfonate Micellar Fluids," *Soc. Pet. Eng. J.*, **25**, 580 (1985).
- Figdore, P. E., "Adsorption of Surfactant on Kaolinite: NaCl v. CaCl_2 Salt Effects," *J. Colloid Interf. Sci.*, **87**(2), 500 (1982).
- Goddard, E. D., and P. Somasundaran, "Adsorption of Surfactants on Mineral Solids," *Croatia Chemica Acta*, **48**(4), 451 (1976).
- Griffith, T. D., "Application of the Ion Exchange Process to Reservoir Preflushes," Paper SPE 7587, 53rd Ann. Fall Tech. Conf. Exhib. SPE, Houston (1978).
- Hirasaki, G. J., "Evaluation of the Salinity Gradient Concept in Surfactant Flooding," Paper SPE 8825, 1st Joint SPE/DOE Symp. EOR, Tulsa (Apr., 1980).
- , "Ion Exchange with Clays in the Presence of Surfactant," *Soc. Pet. Eng. J.*, **22**, 181 (1982).
- Jensen, J. A., and C. J. Radke, "Chromatographic Transport of Alkaline Buffers through Reservoir Rock," Paper SPE 14295, 60th Ann. Tech. Conf. Exhib. SPE, Las Vegas (Sept., 1985).
- Klein, G., "Fixed-bed Ion Exchange with Formation or Dissolution of Precipitate," *Ion Exchange: Science and Technology*, A. E. Rodrigues, ed., NATO ASI Series E: Applied Sciences, No. 107, Nijhoff, Dordrecht (1986).
- Miller, C. W., and L. V. Benson, "Simulation of Solute Transport in a Chemically Reactive Heterogeneous System: Model Development and Application," *Water Resour. Res.*, **19**, 381 (1983).
- OECD-NEA, *Sorption: Modelling and Measurement for Nuclear Waste Disposal Studies*, Summary of an NEA workshop, Paris (June 6-7, 1983).
- Olive, P., *Le Système $\text{CO}_2/\text{H}_2\text{O}/\text{CaCO}_3$. Memento pratique*, Publication de Centre de Recherche Géodynamique, 74203 Thonon les Bains, France (1978).
- Peacock, J. M., and E. Matijevic, "Precipitation of Alkylbenzene Sulfonate with Metal Ions," *J. Colloid Interf. Sci.*, **77**, 548 (1980).
- Pope, G. A., L. N. Lake, and F. G. Helfferich, "Cation Exchange in Chemical Flooding. I: Basic Theory without Dispersion," *Soc. Pet. Eng. J.*, **18**, 418 (1978).
- Reid, V. W., G. F. Longman, and E. Heinerth, "Determination of Anionic Active Detergents by Two-phase Titration," *Tenside*, **4**(9), (1967).
- Rivenq, R., M. Sardin, D. Schweich, and A. Putz, "Sodium Carbonate Preflush: Theoretical Analysis and Application to Chateaufrenard Field Test," Paper SPE 14294, 60th Ann. Tech. Conf. Exhib. SPE, Las Vegas (Sept., 1985).
- Sardin, M., R. Krebs, and D. Schweich, "Transient Mass Transport in the Presence of Physicochemical Interactions: Progressive Modeling and Appropriate Experimental Procedures," *Geoderma*, **38**, 115 (1986).
- Scamehorn, J. F., R. S. Schechter, and W. H. Wade, "Adsorption of Surfactants on Mineral Oxide Surfaces from Aqueous Solutions. I: Isomerically Pure Anionic Surfactants," *J. Colloid Interf. Sci.*, **85**(2), 463 (1982).
- Schweich, D., "Echange d'ions calcium sodium, dissolution de la calcite et précipitation d'un tensio-actif anionique dans un sable argilo calcaire: expériences dynamiques en colonne," *Solid-Liquid Interactions in Porous Media*, Technip, Paris, 63 (1985).
- Schweich, D., and M. Sardin, "Transient Ion Exchange and Solubilization of Limestone in an Oil Field Sandstone: Experimental and Theoretical Wavefront Analysis," *AIChE J.*, **31**(11), 1882 (1985).
- Smith, F. N., "Ion Exchange Conditioning of Sandstones for Chemical Flooding," *J. Pet. Tech.*, **18**, 959 (1978).
- Somasundaran, P., and H. S. Hanna, "Physicochemical Aspects of Adsorption at Solid/Liquid Interfaces. I: Basic Principles," *Improved Oil Recovery by Surfactant and Polymer Flooding*, D. U. Shah, R. S. Schechter, eds., Academic Press, New York (1977).
- Trogus, F. J., T. Sophany, R. S. Schechter, and W. M. Wade, "Static and Dynamic Adsorption of Anionic and Nonionic Surfactants," *Soc. Pet. Eng. J.*, **17**, 337 (1977).
- Villermaux, J., "Génie de la réaction chimique; conception et fonctionnement des réacteurs," *Tech. and Doc.*, Lavoisier, Paris (1982).
- Walsh, M. P., S. L. Bryant, R. S. Schechter, and L. W. Lake, "Precipitation and Dissolution of Solids Attending Flow through Porous Media," *AIChE J.*, **30**, 317 (1984).
- Zundel, J. P. and B. Siffert, "Mécanisme de rétention de l'octylbenzène sulfonate de sodium sur les minéraux argileux," *Solid-Liquid Interactions in Porous Media*, Technip, Paris, 447 (1985).

Manuscript received Jan. 8, 1986, and revision received Feb. 2, 1987.